A new paradigm for the concurrent optimisation of topology and anisotropy fields of variable-stiffness composite structures

Marco Montemurro, Alexandre Mas, Salah-Eddine Zerrouq

CSMA 2024
16ème Colloque National en Calcul des Structures
13-17 Mai 2024, Presqu'île de Giens (Var)

A new paradigm for the concurrent optimisation of topology and anisotropy fields of variable-stiffness composite structures

M. Montemurro[1], A. Mas[1], S. Zerrouq[1]

[1] *Université de Bordeaux, Arts et Métiers Institute of Technology, CNRS, INRA, Bordeaux INP, HESAM Université, I2M UMR 5295, F-33405 Talence, France, marco.montemurro@ensam.eu*

Abstract — This work proposes a new paradigm to tackle the problem of the concurrent optimisation of the topology and anisotropy descriptors of a variable-stiffness composite structure from additive manufacturing technology. The proposed methodology relies on the multi-scale two-level optimisation strategy based on non-uniform rational basis spline (NURBS) entities and the polar formalism. NURBS entities are used to describe both the topology and the distribution of the polar parameters and the thickness over the structure. The effectiveness of the approach is tested on benchmark problems taken from literature.

Keywords — Anisotropy, Topology optimisation, Polar method, Non-uniform rational basis spline entities.

1 Introduction

One of the most difficult optimisation problems in solid mechanics concerns the simultaneous determination of the optimal topology of a continuum and of the optimal distribution and nature of its material. Traditionally, this is achieved at two distinct levels of exchangeable order; structural design and material design.

Structural design aims to achieve the optimal design of a structure/system, taking into account the topology, boundaries and size of the structure. In the conceptual design stage, Topology Optimisation (TO) is commonly utilised, with the goal of identifying the most efficient distribution of a given material in the design domain, and the effective connectivity of its holes, resulting in an optimal performance of the structure. Over the past twenty years, there has been a substantial theoretical and numerical development of TO methods. The most commonly used approaches include density-based methods [1] and the level-set method (LSM) [2].

On a different note, anisotropic continua are often designed using multilayer composite structures with straight fibre format for constant stiffness, or curvilinear fibre format for variable stiffness, potentially with variable thickness and volume fraction. Research has demonstrated that the variable-stiffness design is superior for various properties, including strength [3], buckling load [4], stiffness [5], or a combination of these [6].

One of the most efficient methodologies to design VSC structures is the direct optimisation of the components of the stiffness tensor. In this context, the design problem is often split into two (or more) levels and the resulting strategy is applied to thin-walled VSC structures composed of laminates. Specifically, each VSC laminate is modelled as a plate composed of an equivalent single layer whose point-wise anisotropic behaviour is described through a convenient representation of its characteristic stiffness tensors.

A way to represent anisotropy is through Verchery's polar formalism [7, 8]. This was first proposed in the context of classical laminate theory and later expanded to higher-order equivalent single-layer theories by Montemurro [9, 10]. The polar formalism enables the representation of any plane tensor using tensor invariants, each with a physical meaning related to the various elastic symmetries of the stiffness tensor. The polar formalism has been employed in developing VSCs using the Multi-Scale Two-Level (MS2L) optimisation strategy as outlined by Montemurro et al. [3, 4, 5, 6].

Regarding the concurrent optimisation of topology and anisotropy of VSC structures, Ranaivomiarana et al. [11] considered the problem of the minimisation of the work of external forces of

a structure subjected to homogeneous Dirichlet's Boundary Conditions (BCs) using a density-based TO algorithm, based on the Solid Isotropic with Material Penalisation (SIMP) scheme, to describe the density distribution of the material, and the PPs to describe the anisotropic behaviour. To carry out the solution search, they used the optimality criterion of the alternate directions developed by Allaire et al. [12]. While the obtained solutions do indeed minimise the compliance of the structure, they suffer from several drawbacks that make both the optimality and manufacturability of the solutions questionable. Firstly, a density filter is used to avoid the well-known checker-board effect, but this aspect is not considered when computing the analytical solution for the optimal pseudo-density field $\rho(x)$. Although the density filter helps reducing the checker-board effect, the resulting boundaries are difficult to capture and seem disconnected for some branches. Of course, the resulting solutions are mesh-dependent. Secondly, the authors do not address the problem of the continuity of the PPs fields, which results in a discontinuous solution that cannot be manufactured.

A similar work has been recently presented by Vertonghen et al. [14] where the authors no longer rely on the optimality criterion of the alternate directions [12], but instead use the Method of Moving Asymptotes (MMA) and the Globally-Convergent Method of Moving Asymptotes (GCMMA) [15], to solve in parallel three sub-problems for the optimisation of the pseudo-density field, the orientation angle of the main orthotropy axis and the anisotropic polar moduli. Once again, a filter is applied to the pseudo-density field to reduce the checker-board effect, but no filters are used to enforce the continuity of the PPs, which leads to discontinuous, hence, non-manufacturable solutions. Furthermore, the theoretical framework presented in [14] is characterised by a lack of generality of the problem formulation, which does not consider the maximisation of the structural stiffness in presence of inhomogeneous Neumann-Dirichlet BCs. In this case, as discussed in [16], the work of external forces cannot be used as a measure of the structural stiffness and the notion of generalised compliance (which depends on the total potential energy of the continuum) must be introduced. Finally, the numerical framework presented in [14] lacks generality because it does not consider out-of-plane loads (thus the bending stiffness tensor of the VSC laminate is not optimised) and the possibility of also optimising the thickness distribution of the VSC laminate.

To overcome the above limitations, in this work a general design strategy to face the problem of the concurrent design of topology and anisotropy of VSC structures in the framework of Non-Uniform Rational Basis Spline (NURBS) entities [17] is presented. Specifically, a general formulation of the optimisation problem based on the concept of generalised compliance is provided, as discussed in [16]. In this background, Montemurro et al. developed different algorithms based on NURBS entities for both topology [16] and anisotropy optimisation [3, 4, 5, 6] since they solve many of the issues mentioned above. The basic idea behind the optimisation strategy based on NURBS entities is that each field of design variables of dimension D is modelled by a NURBS entity of dimension $D+1$, and is, hence, uncoupled from the mesh of the Finite Element (FE) model. A NURBS entity is continuous by definition, which solves the issue of continuity of the PPs distribution and of the pseudo-density field. Furthermore, a further advantage of NURBS entities is represented by the local support property. Such a property acts as an implicit filter to reduce/avoid the checker-board effect and to obtain mesh-independent optimised solutions. The theoretical/numerical framework presented in this work is developed in the most general case of VSC structures having variable thickness subjected to inhomogeneous Neumann-Dirichlet BCs and both in-plane and out-of-plane loads. The effectiveness of the proposed approach is tested on meaningful benchmark problems taken from the literature.

2 Concurrent optimisation of the topology and anisotropy fields of a variable-stiffness composite structure

The design of a VSC structure in the framework of the MS2L optimisation strategy is achieved by solving two problems on different levels/scales. The first-level problem aims at determining the optimal topological anisotropy fields satisfying the design requirements of the problem at hand and it is stated at the macroscopic scale (FSDT framework wherein PPs are used to describe the VSC laminate behaviour). The second-level problem aims at searching for, at least, one suitable stacking sequence corresponding to the optimal distribution of pseudo-density and PPs resulting from the first-level problem. The second-

level problem is formulated at the mesoscopic scale of the VSC structure.

In this work, only the first-level problem is addressed. In this section, the basic formalism to correctly state the first-level problem is introduced.

2.1 Topological field design variables

In the NURBS-density-based method [16], NURBS surfaces and hyper-surfaces are used to represent the pseudo-density field. In this way, the topological descriptor is completely uncoupled from the mesh of the FE model, and it is described by a continuous and differentiable function (this aspect allows avoiding/reducing the well-known checker-board issue [1]).

For a 2D problem a 3D NURBS surface is used, whose third coordinate is the pseudo-density field that can be expressed as:

$$\rho(\zeta_1,\zeta_2) = \sum_{i=0}^{n_1}\sum_{j=0}^{n_2} R_{i,j}(\zeta_1,\zeta_2)\,\rho_{i,j}, \tag{1}$$

where n_i+1 is the number of Control Points (CPs) along the i-th direction and $n_{\mathrm{CP}} = (n_1+1)(n_2+1)$ the number of CPs constituting the control net of the surface; $\rho_{i,j}$ is the value of the pseudo-density field at the generic CP, whilst the functions

$$R_{i,j}(\zeta_1,\zeta_2) \coloneqq \frac{w_{i,j}N_{i,p_1}(\zeta_1)N_{j,p_2}(\zeta_2)}{\sum_{k=0}^{n_1}\sum_{l=0}^{n_2} w_{k,l}N_{k,p_1}(\zeta_1)N_{l,p_2}(\zeta_2)} \tag{2}$$

are the piece-wise rational basis functions of the NURBS entity. $w_{i,j}$ is the weight associated to each CP $\rho_{i,j}$, and N_{i,p_k} is the blending function of degree p_k defined recursively by means of the Bernstein's polynomials, as discussed in [17] to which the reader can refer for more details on NURBS entities. The dimensionless parameters ζ_j can be related to the spatial coordinates x_j as:

$$\zeta_j \coloneqq \frac{x_j}{L_j},\ j=1,2,3, \tag{3}$$

where L_j is the characteristic length of the domain along the x_j axis. In this background, the design variables are the pseudo-density $\rho_{i,j}$ of the generic CP and the associated weight $w_{i,j}$ that are collected in the following vector:

$$\boldsymbol{\xi}_1^{\mathrm{T}} = \left(\rho_{i,j}, w_{i,j}\right)_{\substack{1\le i\le n_1\\ 1\le j\le n_2}},\ \boldsymbol{\xi}_1 \in \mathbb{R}^{2n_{\mathrm{CP}}}. \tag{4}$$

2.2 Anisotropy and thickness fields design variables

At the macroscopic scale, the VSC laminate can be modelled as an equivalent homogeneous anisotropic single-layer plate. If the VSC laminate is quasi-homogeneous and orthotropic [9, 10], its local response is described by its thickness t, and three mechanical variables, i.e., the PPs $R_{0K}^{A^*}, R_1^{A^*}$ and $\Phi_1^{A^*}$. Let t_{LB} and t_{UB} denote the lower and upper bounds of the thickness of the laminate, respectively, and let R_0, R_1, Φ_1 be the anisotropic moduli and the second polar angle of the reduced in-plane stiffness matrix $\mathbf{Q}_{\mathrm{in}}$. For optimisation purposes, the following dimensionless quantities are introduced:

$$\tau = \frac{t-t_{\mathrm{LB}}}{t_{\mathrm{UB}}-t_{\mathrm{LB}}},\quad \rho_{0K} = \frac{R_{0K}^{A^*}}{R_0},\quad \rho_1 = \frac{R_1^{A^*}}{R_1},\quad \phi_1 = \frac{2\Phi_1^{A^*}}{\pi}. \tag{5}$$

It is noteworthy that the dimensionless anisotropic moduli ρ_{0K} and ρ_1 in (5) must satisfy the point-wise geometrical feasibility conditions introduced by Vannucci [8] to guarantee they can be matched by, at least, one stacking sequence as a result of the second-level problem [5]. These constraints can be expressed as follows:

$$\begin{cases} -1 \le \rho_{0K} \le 1, \\ 0 \le \rho_1 \le 1, \\ 2\rho_1^2 - 1 - \rho_{0K} \le 0. \end{cases} \tag{6}$$

Izzi et al. [3] introduced a change of variables to remap the feasible domain in the PPs space over the unit square $[0,1]\times[0,1]$. The new set of variables is:

$$(\alpha_0,\alpha_1) \coloneqq \left(\frac{\rho_{0K}-1}{2(\rho_1^2-1)},\rho_1\right), \tag{7}$$

whose converse relation is

$$(\rho_{0K},\rho_1) = \Big(1+2\alpha_0(\alpha_1^2-1),\alpha_1\Big). \tag{8}$$

Taking α_0 and α_1 as design variables instead of ρ_{0K} and ρ_1 makes the design problem easier, since we do not need to introduce the feasibility conditions as explicit constraints, given that all combinations of α_0 and α_1 satisfy the feasibility conditions of Eq. (6). Therefore, the design variables fields describing the macroscopic behaviour of the VSC laminate at the macroscopic scale are $\tau(\zeta_1,\zeta_2)$, $\alpha_0(\zeta_1,\zeta_2)$, $\alpha_1(\zeta_1,\zeta_2)$ and $\phi_1(\zeta_1,\zeta_2)$. Contrary to the pseudo-density field ρ used for TO, only Basis Spline (B-spline) entities are used to describe the spatial variation of these variables, since no oscillations occur when optimising the PPs in the context of the MS2L optimisation strategy [5, 3, 4]. Accordingly, we have:

$$\mu(\zeta_1,\zeta_2) = \sum_{i=0}^{n_1}\sum_{j=0}^{n_2} N_{i,p_1}(\zeta_1)N_{j,p_2}(\zeta_2)\mu_{i,j}, \quad \text{with } \mu = \tau,\alpha_0,\alpha_1,\phi_1. \tag{9}$$

Of course, the design variables are the dimensionless quantities τ, α_0, α_1, ϕ_1 computed at the CPs of the B-spline entity. They can be grouped in the following vector:

$$\boldsymbol{\xi}_2^{\mathrm{T}} = \big(\tau_{i,j},\alpha_{0i,j},\alpha_{1i,j},\phi_{1i,j}\big)_{\substack{1\le i\le n_1\\ 1\le j\le n_2}}, \quad \boldsymbol{\xi}_2 \in \mathbb{R}^{4n_{\mathrm{CP}}}. \tag{10}$$

2.3 Design requirements

Two design requirements are included in the optimisation problem of the VSC structure: the structural stiffness and the lightness. Specifically, the goal is to find the optimal distribution of the topological and anisotropy descriptors that maximises the structural stiffness subject to volume constraint.

At the macroscopic scale, the static equilibrium of the FE model of the VSC structure under inhomogeneous Neumann-Dirichlet BCs [16] reads:

$$\begin{bmatrix} \mathbf{K} & \mathbf{K}_{\mathrm{BC}} \\ \mathbf{K}_{\mathrm{BC}}^{\mathrm{T}} & \tilde{\mathbf{K}} \end{bmatrix} \begin{Bmatrix} \mathbf{u} \\ \mathbf{u}_{\mathrm{BC}} \end{Bmatrix} = \begin{Bmatrix} \mathbf{f} \\ \mathbf{r} \end{Bmatrix}, \tag{11}$$

where $\mathbf{u}\in\mathbb{R}^{N_{\mathrm{DOF}}}$ and $\mathbf{u}_{\mathrm{BC}}\in\mathbb{R}^{N_{\mathrm{BC}}}$ are the vectors of unknown and imposed Degrees of Freedom (DOFs), respectively; $\mathbf{f}\in\mathbb{R}^{N_{\mathrm{DOF}}}$ and $\mathbf{r}\in\mathbb{R}^{N_{\mathrm{BC}}}$ are the vectors of generalised external nodal forces and nodal reactions, respectively. $\mathbf{K}\in\mathbb{R}^{N_{\mathrm{DOF}}\times N_{\mathrm{DOF}}}$, $\mathbf{K}_{\mathrm{BC}}\in\mathbb{R}^{N_{\mathrm{DOF}}\times N_{\mathrm{BC}}}$ and $\tilde{\mathbf{K}}\in\mathbb{R}^{N_{\mathrm{BC}}\times N_{\mathrm{BC}}}$ are the sub-matrices composing the global stiffness matrix $\hat{\mathbf{K}}\in\mathbb{R}^{(N_{\mathrm{DOF}}+N_{\mathrm{BC}})\times(N_{\mathrm{DOF}}+N_{\mathrm{BC}})}$ of the FE model after applying BCs and reordering DOFs. In the case of a VSC structure, the expression of the matrix $\hat{\mathbf{K}}$ in the global reference frame of the FE model is:

$$\hat{\mathbf{K}}(\boldsymbol{\xi}_1,\boldsymbol{\xi}_2) \coloneqq \sum_{e=1}^{N_e}\mathbf{L}_e^{\mathrm{T}}\mathbf{K}_e\mathbf{L}_e = \sum_{e=1}^{N_e}\phi_{Ke}(\boldsymbol{\xi}_1)\mathbf{L}_e^{\mathrm{T}}\int_{A_e}\mathbf{B}_e^{\mathrm{T}}\mathbf{K}_{\mathrm{lam,e}}(\boldsymbol{\xi}_2)\mathbf{B}_e dS\mathbf{L}_e. \tag{12}$$

In Eq. (12), N_e is the number of elements of the mesh of the FE model of the VSc structure, whilst A_e and $\mathbf{K}_{\mathrm{lam,e}}$ are the area and the laminate stiffness matrix [5] of the generic element, respectively. $\mathbf{K}_e\in\mathbb{R}^{N_{\mathrm{DOF,e}}\times N_{\mathrm{DOF,e}}}$ $\mathbf{B}_e\in\mathbb{R}^{8\times N_{\mathrm{DOF,e}}}$ and $\mathbf{L}_e\in\mathbb{R}^{N_{\mathrm{DOF,e}}\times(N_{\mathrm{DOF}}+N_{\mathrm{BC}})}$ are the penalised stiffness matrix, the matrix of the partial derivatives of the shape functions and the connectivity matrix of the generic element, respectively. The definition of $\mathbf{K}_e$ can be easily inferred form Eq. (12), while the other two matrices are defined as:

$$\boldsymbol{\varepsilon}_e = \mathbf{B}_e\mathbf{u}_e, \tag{13}$$

$$\mathbf{u}_e = \mathbf{L}_e\hat{\mathbf{u}}, \quad \hat{\mathbf{u}}^{\mathrm{T}} = \big(\mathbf{u}^{\mathrm{T}},\mathbf{u}_{\mathrm{BC}}^{\mathrm{T}}\big), \tag{14}$$

where $\mathbf{u}_e\in\mathbb{R}^{N_{\mathrm{DOF,e}}}$ is the vector collecting the DOFs of the generic element, whilst $\hat{\mathbf{u}}\in\mathbb{R}^{N_{\mathrm{DOF}}+N_{\mathrm{BC}}}$ is the vector collecting the DOFs of the whole FE model. In Eq. (12), ϕ_{Ke} is the penalty function used

to penalise intermediate values of the pseudo-density field of Eq. (1). In this work, two penalisation schemes are considered, i.e., the well-known SIMP and Rational Approximation of Material Properties (RAMP) schemes that read:

$$\phi_{Ke} = \begin{cases} \rho_e^p & \text{for SIMP,} \\ \frac{\rho_e}{1+q(1-\rho_e)} & \text{for RAMP,} \end{cases} \tag{15}$$

where p and q are the penalty parameters used for SIMP and RAMP schemes, respectively. In this paper they have been set as $p = 3$ and $q = 8$.

As discussed in [16], under inhomogeneous BCs, the requirement on the structural stiffness is expressed through the so-called *generalised compliance* whose expression is:

$$\mathcal{C} \coloneqq \mathbf{f}^{\mathrm{T}}\mathbf{u} - \mathbf{u}_{\mathrm{BC}}^{\mathrm{T}}\mathbf{r}. \tag{16}$$

The physical meaning of $\mathcal{C}$ is immediate. Under homogeneous BCs of the Dirichlet type, i.e., $\mathbf{u}_{\mathrm{BC}} = \mathbf{0}$, maximising the structural stiffness is equivalent to minimise the work of external forces, whilst under null BCs of the Neumann type, i.e., $\mathbf{f} = \mathbf{0}$, the maximisation of the structural stiffness is obtained by maximising the generalised reactions forces $\mathbf{r}$.

The lightness requirement is here expressed via a constraint on the volume of the structure:

$$g \coloneqq \frac{V}{V_{\mathrm{ref}}} - \gamma, \tag{17}$$

where V_{ref} and γ are the reference value of the volume and the volume fraction that should be set by the used, while the expression of the volume of the structure V is

$$V \coloneqq \sum_{e=1}^{N_e} \rho_e \int_{A_e} t dS \approx \sum_{e=1}^{N_e} \rho_e A_e t_e, \tag{18}$$

where t_e is the thickness of the generic element and ρ_e is the pseudo-density field computed at the centroid of the element.

2.4 Problem formulation

In the most general case, the design problem of the VSC structure can be formulated as a Constrained Non-Linear Programming Problem (CNLPP) as:

$$\begin{aligned} &\min_{(\boldsymbol{\xi}_1,\boldsymbol{\xi}_2)} \frac{\mathcal{C}(\boldsymbol{\xi}_1,\boldsymbol{\xi}_2)}{|\mathcal{C}_{\mathrm{ref}}|}, \\ &\text{subject to :} \\ &\begin{cases} \hat{\mathbf{K}}\hat{\mathbf{u}} = \hat{\mathbf{f}}, \\ g(\boldsymbol{\xi}_1,\boldsymbol{\xi}_2) \leq 0, \\ \boldsymbol{\xi}_1 \in [\rho_{\mathrm{LB}}, \rho_{\mathrm{UB}}]^{n_{\mathrm{CP}}} \times [w_{\mathrm{LB}}, w_{\mathrm{UB}}]^{n_{\mathrm{CP}}}, \\ \boldsymbol{\xi}_2 \in [0,1]^{n_{\mathrm{CP}}} \times [0,1]^{n_{\mathrm{CP}}} \times [0,1]^{n_{\mathrm{CP}}} \times [-1,1]^{n_{\mathrm{CP}}}. \end{cases} \end{aligned} \tag{19}$$

In (19), $\mathcal{C}_{\mathrm{ref}}$ is the reference value of the generalised compliance of the structure, whilst $\hat{\mathbf{f}}^{\mathrm{T}} = \left(\mathbf{f}^{\mathrm{T}}, \mathbf{r}^{\mathrm{T}}\right)$ is the vector collecting the generalised forces and reactions of the FE model. ρ_{LB}, ρ_{UB}, w_{LB} and w_{UB} are user-defined bounds on the pseudo-density value and the associated weight at each CP.

To solve problem (19) using gradient-based algorithms, we must compute the gradient of both the generalised compliance and the volume with respect to the different design variables. The formal expression of the gradient of these structural responses has been determined in previous works, see [16] for the partial derivatives with respect to the topological variables, and [5] for the partial derivatives with respect to the PPs and thickness.

3 Numerical results

The effectiveness of the proposed method is illustrated through a benchmark structure withstanding in-plane loads. More test cases will be presented during the speech. The results presented here are obtained by merging the codes SANTO (SIMP And NURBS for Topology Optimisation) [16] and VISION (VarIable Stiffness composItes Optimisation based on NURBS) [5] developed at the I2M laboratory in Bordeaux. Both software are coded in the Python® environment and can be interfaced with any FE code. In this study, the FE code ANSYS® is used to generate the FE model of the structure and to assess the structural responses.

The benchmark structure is modelled using 4-node quadrilateral shell elements (ANSYS SHELL181) with six DOFs per node and its geometry and BCs are shown in Fig 1. The element kinematics is based on the FSDT. The geometrical parameters are: $L_1 = 400$ mm and $L_2 = 200$ mm. The FE model is made

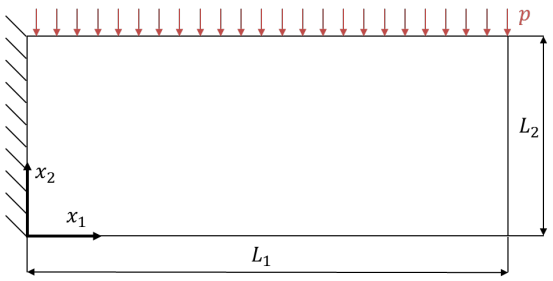

Figure 1: Geometry and BCs of the benchmark structure considered in this work

of $N_e = 120 \times 60$ shell elements; the nodes located at $x_1 = 0$ are clamped, while a force per unit line of intensity $p = 2.5$ Nmm^{-1} oriented towards the negative direction of x_2 axis is applied on the nodes located at $x_2 = L_2$.

The goal of the analyses presented in this section is to investigate the influence of the penalisation scheme used for the element stiffness matrix on the optimised configuration of the VSC structure. For these analyses, the thickness of the VSC structure is not included among the design variables and is set as uniform over the structure as $t = 3$ mm. The material properties of the constitutive lamina of the VSC laminate used for this benchmark can be found in [5].

The PPs are initialised as uniform fields as $\rho_{0K} = 0$, $\rho_1 = 0$, $\phi_1 = 0$, whilst the pseudo-density field is initialised in order to fulfil the constraint on the volume fraction of Eq. (17). The maximum number is set as $N_{\max}^{\text{iter}} = 1000$. The reference value of the compliance (which is the compliance of the initial guess) used to get a dimensionless cost function in Eq. (19) is $\mathcal{C}_{\text{ref}} = 600$ Nmm for SIMP scheme and $\mathcal{C}_{\text{ref}} = 557$ for RAMP scheme. For all the analyses, problem (19) is solved by using a NURBS surface with $n_{\text{CP}} = 90 \times 45$ CPs and degrees of the Bernstein's polynomials equal to $p_1 = p_2 = 2$ for the pseudo-density field, and a B-spline surface with the same integer parameters is used to describe each PP field. Therefore, the overall number of design variables of Benchmark 1 is $n_{\text{var}} = 5n_{\text{CP}} = 20250$.

The optimised configurations of the VSC structure for both penalty schemes are illustrated in Figs. 2-5. Specifically, Fig. 2 illustrates the optimised topology, whilst Figs. 3-5 show the optimised distributions of the PPs over the domain. It is noteworthy that, for each solution, the constraint on the volume fraction of the material phase of Eq. (17) is fulfilled and is almost null at the end of the optimisation process, regardless of the considered combination of optimisation strategy and penalty scheme. This means that the optimised solution is located on the boundary between feasible and infeasible regions of the design space.

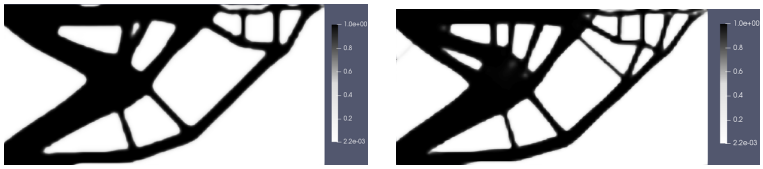

(a) RAMP scheme (b) SIMP scheme

Figure 2: Optimised topology for SIMP and RAMP schemes.

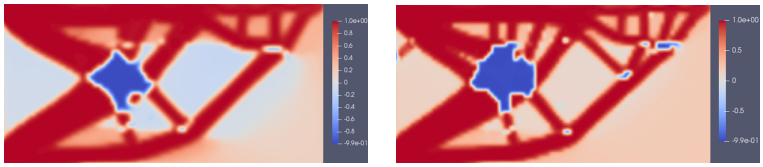

(a) RAMP scheme (b) SIMP scheme

Figure 3: Optimised distribution of ρ_{0K} for SIMP and RAMP schemes.

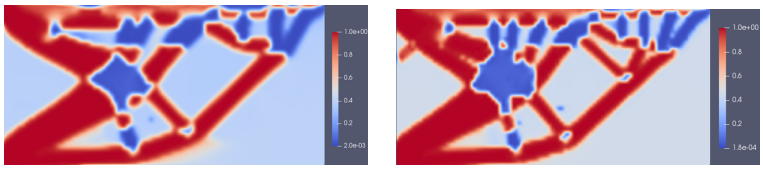

(a) RAMP scheme (b) SIMP scheme

Figure 4: Optimised distribution of ρ_1 for SIMP and RAMP schemes.

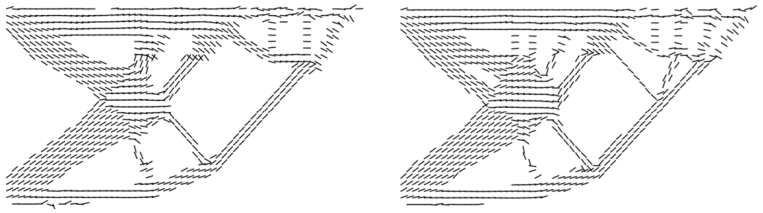

(a) RAMP scheme (b) SIMP scheme

Figure 5: Vector plot of $\Phi_1^{A^*}$ [deg] after threshold operation on the pseudo-density field for SIMP and RAMP schemes

From the analysis of the results shown in Figs. 2-5, the following remarks can be drawn. Firstly, the optimised solutions resulting from the application of the SIMP scheme show a lower generalised compliance $\mathcal{C} = 34.077$ Nmm compared to that obtained with the RAMP scheme, i.e., $\mathcal{C} = 35.782$ Nmm. This is due to the pseudo-density field, which, in the case of the SIMP scheme, converges towards a local minimum with a higher number of topological branches, resulting in a structure that is stiffer than the one obtained in the case of the RAMP scheme.
Secondly, the optimised distribution of ρ_{0K} takes the values -1.0 or 1.0 on the elements wherein $\rho = 1$, whilst ρ_1 is either equal to 1.0 or 0.0 for the same elements. Specifically, as it can be seen from Figs. 3 and 3 three cases can be identified. When $\rho_{0K} = \rho_1 = 1.0$ (red colour in both Figs. 3 and 3 for the same element) the anisotropic polar moduli of the matrix $\mathbf{A}^*$ are equal to those of the constitutive ply. The main orthotropy axis of the matrix $\mathbf{A}^*$ is equal to $\Phi_1^{A^*}$ (see Fig. 5). When $\rho_{0K} = 1.0$ and $\rho_1 = 0.0$ (red colour in Fig. 3 and blue colour in Fig. 4 for the same element) the matrix $\mathbf{A}^*$ of the element is characterised by the square symmetric behaviour [9] (i.e., same stiffness along the main orthtropy axes) and its main orthotropy axes are oriented at $\Phi_1^{A^*}$ and $\Phi_1^{A^*} + \frac{\pi}{2}$, respectively. When $\rho_{0K} = -1.0$ and $\rho_1 = 0.0$ (blue colour in both Figs. 3 and 4 for the same element) the matrix $\mathbf{A}^*$ still exhibits square symmetric behaviour, but the main orthotropy axes are oriented at $\Phi_1^{A^*} + \frac{\pi}{4}$ and $\Phi_1^{A^*} + \frac{3\pi}{4}$. This situation arises in those elements showing a high in-plane shear stress, specifically in the thick region at the centre of the structure.

4 Conclusions

In this paper a general theoretical/numerical framework for the simultaneous optimisation of the topology and the anisotropy of variable-stiffness composite structures is presented. The proposed approach is based on non-uniform rational basis spline entities to describe the topological and anisotropy descriptors. The polar parameters have been used to describe the anisotropy of the variable-stiffness composite

structure at the macroscopic scale because they are directly related to the elastic symmetries of the stiffness matrices of the laminate. In this way, it is possible to optimise not only the mechanical behaviour of the laminate at each point of the design domain, but also the nature of the elastic symmetry as well as the orientation of the main symmetry axes.
The effectiveness of the proposed approach will be discussed during the speech and further examples including out-of-plane loads and local thickness optimisation will be illustrated and discussed.

References

[1] M. P. Bendsøe, O. Sigmund, Topology optimization: theory, methods, and applications, second edition, corrected printing Edition, Engineering online library, Springer, Berlin Heidelberg, 2011.

[2] G. Allaire, F. Jouve, A.-M. Toader, Structural optimization using sensitivity analysis and a level-set method, Journal of Computational Physics 194 (1) (2004) 363–393.

[3] M. I. Izzi, A. Catapano, M. Montemurro, Strength and mass optimisation of variable-stiffness composites in the polar parameters space, Structural and Multidisciplinary Optimization 64 (4) (2021) 2045–2073.

[4] G. Fiordilino, M. Izzi, M. Montemurro, A general isogeometric polar approach for the optimisation of variable stiffness composites: Application to eigenvalue buckling problems, Mechanics of Materials 153 (2021) 103574.

[5] M. Montemurro, A. Catapano, A general B-Spline surfaces theoretical framework for optimisation of variable angle-tow laminates, Composite Structures 209 (2019) 561–578.

[6] M. I. Izzi, M. Montemurro, A. Catapano, Variable-stiffness composites optimisation under multiple design requirements and loads, International Journal of Mechanical Sciences 258 (2023) 108537.

[7] G. Verchery, Les Invariants des Tenseurs d'Ordre 4 du Type de l'Élasticité, in: J.-P. Boehler (Ed.), Mechanical Behavior of Anisotropic Solids / Comportment Méchanique des Solides Anisotropes, Springer Netherlands, Dordrecht, 1982, pp. 93–104.

[8] P. Vannucci, Anisotropic Elasticity, Vol. 85 of Lecture Notes in Applied and Computational Mechanics, Springer Singapore, Singapore, 2018.

[9] M. Montemurro, An extension of the polar method to the First-order Shear Deformation Theory of laminates, Composite Structures 127 (2015) 328–339.

[10] M. Montemurro, Corrigendum to "An extension of the polar method to the First-order Shear Deformation Theory of laminates" [Compos. Struct. 127 (2015) 328-339], Composite Structures 131 (2015) 1143–1144.

[11] N. Ranaivomiarana, F.-X. Irisarri, D. Bettebghor, B. Desmorat, Concurrent optimization of material spatial distribution and material anisotropy repartition for two-dimensional structures, Continuum Mechanics and Thermodynamics 31 (1) (2019) 133–146.

[12] Z. B. Grégoire Allaire, F. Jouve, The homogenization method for topology and shape optimization. single and multiple loads case, Revue Européenne des Éléments Finis 5 (5-6) (1996) 649–672.

[13] A. Vincenti, B. Desmorat, Optimal Orthotropy for Minimum Elastic Energy by the Polar Method, Journal of Elasticity 102 (1) (2011) 55–78.

[14] L. Vertonghen, F.-X. Irisarri, D. Bettebghor, B. Desmorat, Gradient-based concurrent topology and anisotropy optimization for mechanical structures, Computer Methods in Applied Mechanics and Engineering 412 (2023) 116069.

[15] K. Svanberg, A Class of Globally Convergent Optimization Methods Based on Conservative Convex Separable Approximations, SIAM Journal on Optimization 12 (2) (2002) 555–573.

[16] M. Montemurro, On the structural stiffness maximisation of anisotropic continua under inhomogeneous Neumann-Dirichlet boundary conditions, Composite Structures 287 (2022) 115289.

[17] L. Piegl, W. Tiller, The NURBS Book, Monographs in Visual Communication, Springer Berlin Heidelberg, Berlin, Heidelberg, 1997.